
Vehicle System Dynamics
Publication details, including instructions for authors and subscription information:
http://www.tandfonline.com/loi/nvsd20

# Design of electromagnetic shock absorbers for automotive suspensions

Nicola Amati [a], Andrea Festini [b] & Andrea Tonoli [a]

[a] Mechanics Department, Mechatronics Laboratory, Politecnico di Torino, Torino, Italy

[b] Mechatronics Laboratory, Politecnico di Torino, Torino, Italy

Available online: 15 Aug 2011

To cite this article: Nicola Amati, Andrea Festini & Andrea Tonoli (2011): Design of electromagnetic shock absorbers for automotive suspensions, Vehicle System Dynamics, 49:12, 1913-1928

To link to this article: http://dx.doi.org/10.1080/00423114.2011.554560

*Vehicle System Dynamics*
Vol. 49, No. 12, December 2011, 1913–1928





# Design of electromagnetic shock absorbers for automotive suspensions

Nicola Amati[a]*, Andrea Festini[b] and Andrea Tonoli[a]

[a]*Mechanics Department, Mechatronics Laboratory, Politecnico di Torino, Torino, Italy;*
[b]*Mechatronics Laboratory, Politecnico di Torino, Torino, Italy*

(*Received 3 December 2010; final version received 6 January 2011; first published 15 August 2011*)

Electromechanical dampers seem to be a valid alternative to conventional shock absorbers for automotive suspensions. They are based on linear or rotative electric motors. If they are of the DC-brushless type, the shock absorber can be devised by shunting its electric terminals with a resistive load. The damping force can be modified by acting on the added resistance. To supply the required damping force without exceeding in size and weight, a mechanical or hydraulic system that amplifies the speed is required. This paper illustrates the modelling and design of such electromechanical shock absorbers. This paper is devoted to describe an integrated design procedure of the electrical and mechanical parameters with the objective of optimising the device performance. The application to a C class front suspension car has shown promising results in terms of size, weight and performance.

**Keywords:** active suspension; mechatronics; electromagnetics; semi-active suspension

## 1. Introduction

Vehicle suspensions are usually equipped with hydraulic shock absorbers operating in a passive, semi-active or active mode. The passive configuration is efficient for standard performance because it is simple and cost-effective, therefore it is widely used. Hydraulic systems with electromechanical valves are used in some C- and D-segment models (compact and mid-size cars) to obtain better handling and comfort. Active devices with external power systems have few applications mostly related to top class, sports cars and research prototypes to ensure optimal comfort and handling performances in the most wide range of manoeuvring conditions [1,2]. The above considerations underline how the hydraulic technology is widely consolidated for the vibration suppression and handling control in transportation systems. It is characterised by high power density, mechanical simplicity [3] and low costs. Nevertheless, the high sensitivity of the performance to the operating conditions, the low predictability of the characteristics, the tuning difficulties of the working parameters [4], and the ageing and wear of the fluid are not negligible drawbacks. These effects are emphasised if the actuator is controlled in a semi-active or active mode.

*Corresponding author. Email: nicola.amati@polito.it

ISSN 0042-3114 print/ISSN 1744-5159 online

http://dx.doi.org/10.1080/00423114.2011.554560
http://www.tandfonline.com

By converse, the 'X-by wire' technology for steering, braking or shifting is becoming more competitive in a contest where many on board systems are becoming more electrical. The main advantages are the high flexibility of the electromechanical actuators to adapt their performances to the operating conditions, the lower sensitivity to the environmental effects and operating conditions such as frequency and temperature, and the energy savings that they can allow.

Some attempts to apply the 'X-by wire' technology to automotive suspension systems have been made in the past. der Knaap *et al*. [5] and der Knaap and Pacejka [6] proposed an active suspension equipped with an electromagnetic actuator to suppress the roll and pitch motion. The system is configured to control the spring force by varying the attachment point of the spring to the wheel hub using an electromagnetic actuator. Weeks *et al*. [7,8] proposed the use of electromagnetic shock absorbers to isolate the passenger compartment of military vehicles and metropolitan transit buses. They proposed an active electromagnetic device in conjunction with an air spring to reduce the vertical motion of the sprung mass and the hopping of the wheel. The experimental results show that the solution allows a considerable reduction of the waste of power for off-road vehicles negotiating in rough terrains. The larger bandwidth of the electromagnetic actuators makes them more suitable to this application than the hydraulic ones [7]. By converse, the smaller power and force density require an in-depth analysis of the required active forces to avoid excessive weight. The obtained results are at any rate very promising even if limited to off-road applications.

Since the beginning of the 1980s, Miller [9] and Jolly and Margolis [10] have been demonstrating that semi-active devices connecting the sprung and unsprung masses are very promising if the goal is the reduction of the acceleration of both masses. The results are close to those observed for fully active skyhook dampers in the frequency range of interest.

Karnopp [11,12] proposed the concept of a passive or semi-active electromechanical damper based on a linear electric motor with permanent magnets (PMs) whose electric terminals are shunted by a resistance. The damping coefficient can be controlled by acting on the shunt resistance, according to the vehicle dynamics. The proposed configuration can be considered as one of the most powerful semi-active systems fitting the promising performances highlighted in [9,10]. Inoue *et al*. [13] proposed a configuration using a resonant shunt damper, describing the damping as the function of the frequency, and including inductance and capacitance in the shunted circuit to modify the mechanical characteristics of the electrical machine by purely passive means. A solution based on a linear configuration has also been proposed by Ebrahimi *et al.* [14] and Bae *et al.* [15], although interesting in the usage of PMs to generate the flux, and the solid copper conductor does not allow any tuning of the damping coefficient. Compared with the standard hydraulic solutions, the advantages of the electromechanical damper are as follows: (1) the simplicity and the reliability of the configuration; (2) the small sensitivity to environmental parameters such as temperature and ageing; (3) the small static friction and (4) the larger bandwidth. Additionally, the electromechanical nature of the device opens possibilities that are very difficult to obtain by hydraulic systems: (1) with an external electrical power, they can be used in active mode (as described in [7,8]), and (2) the reversibility of the electrical machine allows to devise regenerative solutions. The energy stored in passive mode can be used in active mode to control handling dynamics. By converse, the large weight (and cost) that characterises all electromechanical solutions proposed in the literature puts their potentialities in a dark shade and makes them unacceptable compared with the hydraulic ones.

The aim of this paper is to propose passive or semi-active electromechanical shock absorbers exploiting rotational electric PM machines in order to obtain a good compromise between performances and weight. To this end, a configuration where a rotational motor is connected to a mechanical transmission (e.g. a ball screw [16], a gearbox and a lever, or an electrohydrostatic

transmission [17]) that converts the linear motion into rotational motion is considered to avoid the large weight that characterises the solutions based on linear motors [12].

The innovative aspects of this design technique are as follows: (1) novel optimisation of the design parameters, evidencing that the design is driven by a few number of parameters involving the mechanical and the electrical variables; (2) system model taking into account the small and large amplitude motions during transient and (3) comparison of damping-to-weight ratio relative to other solutions present in the literature.

The application to a C-segment car suspension has been evaluated by modelling and designing in detail a complete retrofit shock absorber. This solution shows promising results in terms of sprung/unsprung masses, sizes and performances.



## 2. Working principle

The passive electromechanical damper described in the following sections is based on a brushless electric motor with PMs whose electric terminals are shunted by a resistive load. Compared with the brushed motors, the brushless ones guarantee higher reliability and performance, and possibly a lower cost in the case of resistive shunting. The complex sensing and control needed to drive them as motors are not needed in this case.

As described in [18], the shunted motor generates an electromagnetic torque $T_{\mathrm{em}}$ that counteracts rotation. Assuming the rotational speed $\Omega$ as constant, the expression of the torque is similar to that of an induction motor:

$$T_{\mathrm{em}}(\Omega(s=0)) = \frac{c_\omega}{1+(p\Omega(s=0))^2/\omega_{\mathrm{p}}^2}\Omega(s=0),$$
$$\text{where} \quad c_\omega = \frac{K_{\mathrm{t}} \cdot K_{\mathrm{e}}}{R} \quad \text{and} \quad \omega_{\mathrm{p}} = \frac{R}{L}. \tag{1}$$

The terms $K_{\mathrm{t}}$ and $K_{\mathrm{e}}$ are the torque and the back electromotive force constants, and $R$ and $L$ are the resistance and inductance of the windings associated with each of the $p$ pole pairs of the two-phase equivalent model for the electrical machine. For 'electrical' angular speeds $p\Omega$ smaller than the $R/L$ pole $\omega_{\mathrm{p}}$ ($p\Omega \ll \omega_{\mathrm{p}}$), the torque to speed characteristic is linear, with a good approximation. This suggests the use of the device as a viscous damper of coefficient $c_\omega$. The damping coefficient $c_\omega$ can be varied by acting on the shunt resistance (Equation (1)); the lower the resistance, the higher the damping. This is similar to what is obtained in hydraulic dampers by changing the diameter of the orifices that laminate the oil flow. In the case of the electromechanical damper, the availability of fast power electronic devices at a low cost allows to implement the variable damping coefficient feature at a competitive price relative to the hydraulic solution.

By converse, if the electrical speed is larger than the pole frequency ($p\Omega \gg \omega_{\mathrm{p}}$), the torque decreases with the angular speed $\Omega$ following a constant power characteristic. The reduction of the reaction torque for high speeds is an attractive feature for automotive shock absorber applications. High damping coefficients are needed, on the one hand, to contrast the small compression/extension speeds (in the range of 0.1–0.2 m/s) involved during cornering and braking, and to limit the resulting body roll and pitch. On the other hand, to minimise the transmission to the chassis of forces corresponding to the high compression/extension speeds (in the 1–2 m/s range) induced during obstacle negotiation and improve comfort, a low value of damping is required.

With reference to Equation (1), the assumption that the angular speed is constant will never be met in automotive suspensions because the motion is always oscillatory with multi-harmonic content. Nevertheless, Amati *et al.* [19] and Tonoli [18] demonstrated that the

torsional damping coefficient $c_\omega$ of 1 is valid also under transient conditions, provided that the angular speed $\Omega$ and its dominant harmonic components are both below $\omega_p$.

If the angular speed oscillates with a small amplitude and a frequency content that is not negligible relative to $\omega_p$, the electromagnetic torque can be characterised by the transfer function between the input speed $\Omega$ and the output torque $T_{em}$. This transfer function is the mechanical impedance of the damper ($Z_m(s)$). Its expression in the Laplace domain is as follows:

$$Z_m(s) = \frac{T_{em}(s)}{\Omega(s)} = \frac{c_\omega}{1 + s/\omega_p}, \tag{2}$$

where $s$ is the Laplace variable. For frequencies ($s = j\omega$) lower than the pole frequency, the device acts as a *viscous damper* of damping coefficient $c_\omega$ given by Equation (1). By converse, for frequencies higher than the pole frequency, the torque is proportional to the relative angle. The device acts as a *mechanical spring* of stiffness

$$k_\theta = \frac{K_t K_e}{L}. \tag{3}$$

The band-limited nature of the mechanical impedance is a positive feature to allow damping of the relevant dynamics while limiting the high-frequency transmissibility. The pole frequency must be chosen in this case as a trade-off between the need to give enough damping to the low-frequency dynamics and than to decrease the high-frequency transmissibility. Considering Equation (2) from a purely mechanical point of view, the mechanical impedance is that of the series of a viscous damper of damping coefficient $c_\omega$ and a spring of stiffness $k_\theta$.

Even if Equations (1) and (2) apply for the multi-phase linear motors with PMs, a preliminary study evidenced that linear electric motors still have several disadvantages in terms of weight, size and power dissipation when compared with the rotating ones. This is because in the case of small amplitude displacements, a reduced part of a linear electric motor is active. Nevertheless, its total length must be designed to allow the maximum displacement, even if it occurs for a limited time. Most of the parts of the linear motors are then not used most of the time. By converse, in rotational motors, all the magnetic and conductor materials contribute to the torque generation; this makes them lighter than the linear ones to obtain the same linear damping value. Additionally, rotating electric motors are based on a more consolidated design practice and technology background.

The solution in Figure 1 shows a sketch of the proposed linear electromechanical damper. A shunted electric motor with PMs is connected to a ball screw that converts the linear motion into rotation. For simplicity reasons, the electric motor is represented as a brush motor with its two electric terminals connected to a lumped resistor and inductor. In practice, it will be a brushless motor whose two or three phases will be shunted by a resistive network.

For what the conversion from linear motion into rotative motion is concerned, many alternatives are possible for the ball screw, each with its advantages and drawbacks. A purely

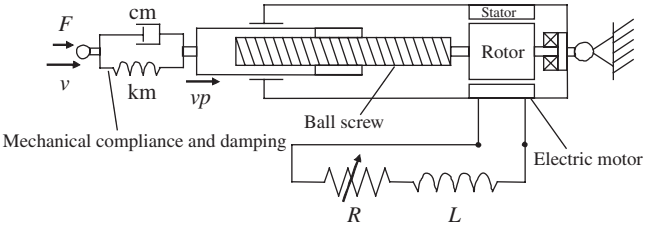


Figure 1. Sketch of the electromechanical shock absorber.

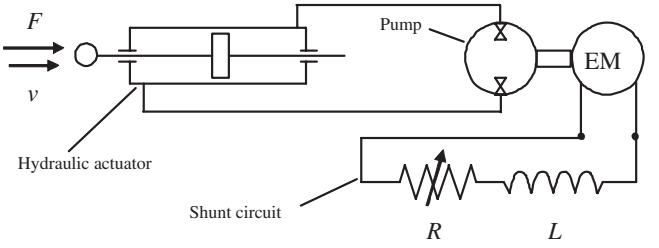


Figure 2. Sketch of the electrohydrostatic shock absorber.



mechanical one could involve a lever of suitable length and a gearbox to amplify the angular speed of the lever before going into the motor. Due to the compact size, this configuration is interesting for rear automotive or motorcycle trailing arm suspensions, while the ball screw solution seems to be more convenient for strut- type front suspensions. Another alternative could be to use an hydraulic piston connected to a fixed displacement pump driving the rotor of the electric motor (electrohydrostatic transmission, Figure 2) [17].

With reference to Figure 1, resistance $R$ includes the contributions of the windings ($R_m$) and of the external resistors ($R_{ext}$) allowing to tune the damping coefficient ($R = R_m + R_{ext}$). Since the effect of inductance $L$ is usually unwanted, no external contribution is added to that of the motor.

As shown in [19], the contribution of the masses and inertias to the dynamic response of the damper cannot be neglected. The most important effect is that of the rotating parts; at high frequency, they counteract the motion of the piston with a force that increases with frequency. This effect is the one typical of the so-called inerter, a device that supplies an inertia force that is proportional to the relative acceleration between two points; if needed, this force could be reduced by adding a compliant element in series with the damper. This is represented in Figure 1 as a spring-damper element connected to the piston rod. This compliance could also account for the compliances of the mechanical parts that realise the transformation from linear motion into rotational motion.

Figure 3 shows the bond graph model of the electromechanical damper. The *assumptions* at the base of the model are the following:

(1) The damper is driven with a speed $v$, and its response is force $F$.
(2) The mechanical and electrical subsystems are modelled with lumped parameters.
(3) The dissipations in the ball screw, in the bushings and in the bearings are modelled as a linear viscous damper of coefficient $c_s$.

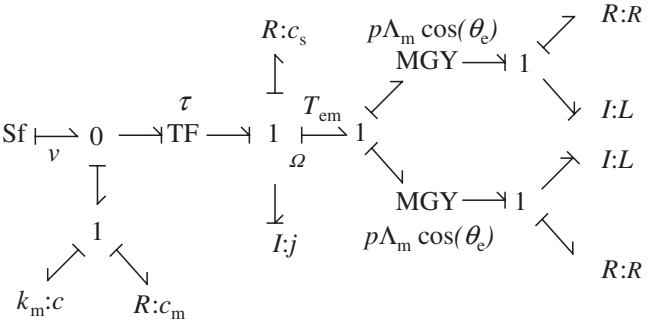


Figure 3. Bond graph model of the electromechanical shock absorber.

(4) The inertias of the moving part (piston and nut of the ball screw) are merged to that of the rotating parts.
(5) The brushless motor has $p$ pole pairs and is modelled with its a–b equivalent [20].
(6) The reluctance effects (cogging) in the motor are neglected.
(7) The iron losses in the motor are neglected.

The conversion from linear motion into rotational motion is modelled in the bond graph by transformer TF of coefficient $\tau$ (rad/m). The common flow node (type 1 node) to the right of the transformer represents the angular speed $\Omega$ of the screw and of the rotor.

The next common flow node makes the angular speed $\Omega$ common to all $p$ pole pairs and adds their torque contributions. The two electrically orthogonal windings associated with each pole pair are modelled by two modulated gyrators (MGYs). The $p$ pole pairs are subject to the same speed and, being magnetically and electrically identical, make contributions to the torque. Their cumulative effect is, therefore, accounted for by factor $p$ multiplying the electromechanical conversion factor of the single pole pair ($\Lambda_m$) in the modulated gyrators. As a single winding experiences $p$ cycles of the magnetic field of the stator, for each complete rotation of the rotor ($\theta = 2\pi$), the angle that modulates each gyrator is the electrical angle $\theta_e = p\theta$ instead of the rotor angle. The resistance and self-inductance in series to each winding are represented by the $R$ and $I$ elements connected to the common flow node ($1 : i$) to the right of each gyrator.

The model of the shunted motor included in the bond graph in Figure 3 can be used to study the electromechanical torque for rather general angular speeds, including constant speed and small amplitude vibrations. The torque of Equation (1) is relative to constant speed conditions and the mechanical impedance of Equation (2) to small amplitude vibrations, to cite just two limit cases.

As shown in the considerations following Equation (2), for vibrations involving an angular speed much smaller than the electrical dynamics ($|\Omega| < p\omega_p$), the shunted electric motor behaves as the series of a viscous damper and a spring. As has been mentioned already, the angular speed $\Omega$ and the oscillation frequency $\omega$ are two different entities. The electromechanical model in Figure 3 can be transformed in the purely mechanical system in Figure 4, provided that one of the ends of the shock absorber is fixed. To this end, the effects of the transformer have been included in the equivalent inertia ($m_{eq}$), damping ($c_{seq}$) and stiffness ($k_{em}$):

$$m_{eq} = \tau^2 J + m_t, \quad c_{em} = \tau^2 \frac{K_t K_e}{R}, \quad c_{seq} = \tau^2 c_s \quad k_{em} = \tau^2 \frac{K_t K_e}{L}, \tag{4}$$

where $J = (J_{em} + J_s)$ is the moment of inertia of the rotating parts including the rotor of the electric motor ($J_{em}$) and the screw ($J_s$). $m_t$ is the mass of the translating parts, and $R$ and $L$ are the resistance and inductance of the windings associated with each pole pair. In the case of the two-phase electric motor adopted in the bond graph, the torque and the back electromotive

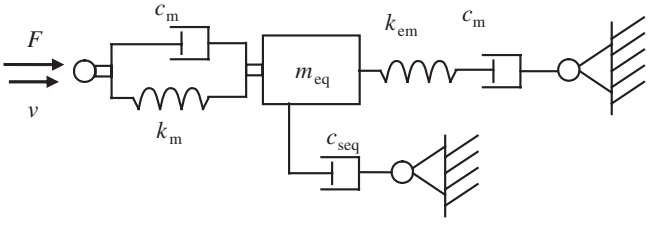


Figure 4. Purely mechanical analogue.

force constants are the same

$$K_t = K_e = p\Lambda_m, \tag{5}$$

where $\Lambda_m$ is the amplitude of the magnetic flux produced by the PMs of the rotor and linked to the stator windings.

The dynamic behaviour of the damper in Figure 4 can be characterised in the frequency domain by its mechanical impedance: that is, the transfer function between input speed $v$ and corresponding force $F$:

$$\frac{F}{v} = \frac{s + (1/m_{eq})(c_{seq} + (c_{em}/(1 + s/\omega_p))}{s^2 + (1/m_{eq})(c_{seq} + c_{em}/(1 + s/\omega_p))s + \omega_m^2}(k_m + sc_m), \tag{6}$$

where $\omega_p$ is the *RL* pole frequency and $\omega_m$ is the undamped mechanical resonant frequency with open circuited electric terminals of the motor. The last involves the motion of the rotating parts and the deformation of the spring ($k_m$) in series with the piston:

$$\omega_p = \frac{R}{L} = \frac{k_{em}}{c_{em}}, \quad \omega_m = \sqrt{\frac{k_m}{m_{eq}}}. \tag{7}$$

For frequencies well below the zero and pole dynamics, the mechanical impedance reduces to that of a viscous damper of coefficient $c_{eq} = c_{seq} + c_{em}$.

The mechanical impedance can be simplified by taking the following design considerations into account:

- The electrical pole $\omega_p$ is set at a value high enough to cover the desired damping range.
- The mechanical losses in the screw and in the piston bushings are a parasitic effect that must be kept as small as possible to allow control of the electromechanical force generated by the damper. To this end, $c_s \ll c_\omega$.

The simplified form of the mechanical impedance is then

$$\frac{F}{v} = c_{em}\frac{\omega_m^2\omega_p}{\omega_{0em}^2\omega_{0m}}\frac{(s + \omega_{0m})(s^2 + 2\zeta_{0em}\omega_{0em}s + \omega_{0em}^2)}{(s^3 + s^2\omega_p + 2\omega_m^2 s + \omega_m^2\omega_p)}, \tag{8}$$

where the zero frequencies and damping factor are

$$\omega_{0m} = \frac{k_m}{c_m}, \quad \omega_{0em} = \sqrt{\frac{k_{em}}{m_{eq}}}, \quad \zeta_{0em} = \frac{\sqrt{m_{eq}k_{em}}}{2c_{em}}. \tag{9}$$

The numerator of the mechanical impedance of Equation (8) is characterised by three zeros. The first is a real zero related to the mount stiffness and damping ($\omega_{0m}$). The other two ($\omega_{0em}$) are related to the electromechanical interaction. The substitution of the second expression of Equations (9) in the third allows one to write the zero damping $\zeta_{0em}$ as a function of the pole frequency $\omega_p$ and the electromechanical zero frequency $\omega_{0em}$:

$$\zeta_{0em} = \frac{\omega_p}{2\omega_{0em}}. \tag{10}$$

From Equation (10), and with reference to the data given in the appendices, reported in Table 6, providing a numerical example, it follows that

- if $\omega_{0em} > \omega_p/2$, the zero damping is smaller than unity ($\zeta_{0em} < 1$), and the mechanical impedance has two complex and conjugate zeros due to the electromechanical stiffness ($k_{em}$) and to the equivalent mass of the moving parts ($m_{eq}$);

- by converse, if $\omega_{0em} < \omega_p/2$, the zero damping is larger than unity ($\zeta_{0em} > 1$) and the electromechanical zeros are real and negative, one of them is at a frequency lower than the pole frequency.

The denominator of Equation (8) is characterised by three poles. With parameter values that are realistic for automotive applications, two of them are complex conjugate and one is real. The first one is approximately half the $RL$ constant of the electrical circuit ($\omega_p/2$). The other two are complex conjugate with frequency $\omega_m$.

At frequencies well below all zero and pole dynamics, the mechanical impedance is that of a viscous damper of damping coefficient $c_{em}$. By converse, above them, the impedance is that of the viscous damper included in the mount ($c_m$). At intermediate frequencies, the shape of the transfer function depends on the relative position between the zeros and the complex conjugate poles. Figure 7 is relative to the case when $\omega_p/2 < \omega_{0em} < \omega_m$. Apart from the complex conjugate zero–pole dynamics, in the intermediate frequency range, the mechanical impedance shows a mean $-20$ dB/dec slope. This figure is relative to the study presented in Section 4. This indicates an equivalent behaviour of a spring of stiffness $k_{em}$. In Table A1, reported in the appendices, the characteristics of the designed damper are reported in order to provide a numerical example.

## 3. Electromechanical design

The objective of the design could be to obtain the required maximum damping $c_{em}$ while keeping the equivalent mass $m_{eq}$ as small as possible. The right amount of torsional damping has to be defined according to vehicle dynamics, while minimising the equivalent mass will lead to the minimum inertial effects.With reference to Equation (4), the equivalent mass $m_{eq}$ and the damping coefficient $c_{em}$ are proportional to the square of the transmission ratio $\tau$. Focusing on the contribution to the mass and damping made just by the electrical machine and excluding the contribution of the ball screw and moving mass, the ratio $c_{em}/m_{eq}$ is then the same as the ratio between torsional damping and the moment of inertia of the rotor:

$$\frac{c_{em}}{m_{eq}} = \frac{c_\omega}{J_{em}}, \tag{11}$$

the higher this ratio, the lower the inertial effects. The objectives of this section are as follows: (1) to find a relationship between the torsional damping and the rotor moment of inertia, and (2) to evaluate the mass of the electrical machine.

This is done under the following assumptions, considered acceptable in the design phase of every PM machine:

(1) The magnetic field is the same in all sections perpendicular to the rotor axis of active length $l$.
(2) The stator winding distribution $f(\alpha)$ is a sinusoidal function of the description angle $\alpha$ of the stator:

$$f(\alpha) = \frac{N}{2}\cos\alpha, \tag{12}$$

$N$ is the number of turns per pole pair and per phase.

(3) The magnetic flux density $B_m(\alpha - p\theta)$ produced by the PMs at the air gap has a square wave distribution:

$$B_m(\alpha - p\theta) = B_0 \sum_{n=1}^{\infty} \frac{4}{\pi n} \cos[n(\alpha - p\theta)], \tag{13}$$

where $B_0$ is the amplitude of the square wave and $\theta$ is the angular position of the rotor (mechanical angle).

(4) The total volume of the copper $V_{cu}$ in the stator windings is constant.

For a two- or three-phase brushless motor with a sinusoidal electromotive force (AC brushless), the constants $K_t$ and $K_e$ of Equation (1) can be expressed as a function of the number of pole pairs $p$ and of the magnetic flux $\Lambda_m$:

$$\begin{aligned} K_t &= \frac{m}{2} p \Lambda_m \\ K_e &= p \Lambda_m \end{aligned} \quad (m = 2, 3 \text{ motor phases}). \tag{14}$$

For a two-phase motor ($m = 2$), the two constants are the same, as in the bond graph in Figure 3. For a three-phase motor, as the current considered in obtaining the torque is the *phase current* and there are *three active phases*, the torque constant is affected by a factor 3/2.

Assumptions 1, 2 and 3 allow to compute the flux $\lambda_m$ linked by a phase as the integral on the description angle $\alpha$ in the range $-\pi, \pi$ [21]

$$\lambda_m(\theta) = rl \int_{-\pi}^{\pi} f(\alpha) B_m(\alpha - p\theta)\, d\alpha. \tag{15}$$

The flux linkage $\lambda_m(\theta)$ is obtained by the substitution of Equations (12) and (13) in Equation (15). If only the first harmonic of the magnetic flux density $B_m$ (Equation (13)) is considered, the magnetic flux and its amplitude become

$$\lambda_m(\theta) = \Lambda_m \cos(p\theta), \quad \text{with } \Lambda_m = 2rlNB_0. \tag{16}$$

As explained in [19], the substitution of $\Lambda_m$ and resistance $R$ in $c_\omega$ of Equation (1) allows to compute the torsional damping coefficient as a function of the rotor radius and active length:

$$c_\omega = \Gamma_c r^4 l. \tag{17}$$

Parameter $\Gamma_c$ is a function of the geometric proportions of the motor, characteristics and amount of conductors and PMs:

$$\Gamma_c = \frac{2\pi^2 \sigma B_0^2}{K_{conn.} N_s} H \left(1 + \frac{\delta}{r}\right)^2, \tag{18}$$

in the above equation, $\sigma$ is the conductivity of the winding, $\delta$ is the radial gap between rotor and stator, and $N_s$ is the number of slots (and teeth) in the stator. The nondimensional parameter $H$ takes the geometric proportions of the stator slots and teeth into account, and $K_{conn}$ takes the size of the end windings relative to the active length of the motor into account. Their expressions are reported in Appendix 2.

The static damping coefficient is the same for a two-phase or a three-phase motor. Even if the two-phase configuration could be more convenient, as it requires a smaller number of power electronic components, the three-phase configuration is usually adopted instead to reduce the torque ripple. Sinusoidal motors are usually better suited than trapezoidal ones for the same reason.

From a mechanical point of view, the moment of inertia ($J_{\mathrm{em}}$) of the rotor is computed as a function of its radius and active length, considering an equivalent mass density $\rho$:

$$J_{\mathrm{em}} = \frac{\pi}{2}\rho r^4 l. \tag{19}$$

The moment of inertia of Equation (19) and the torsional damping of Equation (17) have the same dependence on radius $r$ and active length $l$. Their ratio is, therefore, just a function of the motor shape and materials:

$$\frac{J_{\mathrm{em}}}{c_\omega} = \frac{\pi}{2}\frac{\rho}{\Gamma_c}. \tag{20}$$

If only the contribution of the electric motor is considered in the equivalent mass and damping (Equation (4)), Equation (20) allows to conclude that the ratio between the equivalent mass ($m_{\mathrm{eq}}$) and linear damping coefficient ($c_{\mathrm{eq}}$) is also constant. This is a very important result from the design point of view. Once the equivalent damping is specified, the equivalent mass ($m_{\mathrm{eq}}$) brought in the suspension by the inertia of the motor is just a function of the motor design ($\rho$, $\Gamma_c$). The only way to reduce it is by improving constant $\Gamma_c$.

The overall mass of the electric motor $m_{\mathrm{em}}$ is the other important mechanical property of the damper. Similar to what has been done for the damping coefficient of Equation (17), it can be expressed as a function of the rotor radius and active length:

$$m_{\mathrm{em}} = \Gamma_{\mathrm{m}} r^2 l, \tag{21}$$

where the dimensional parameter $\Gamma_{\mathrm{m}}$ is a function of the aspect ratios of Appendix 2 and of the mass densities.

The substitution of the term $r^2 l$ of Equation (21) into Equation (17) allows to link the torsional damping coefficient $c_\omega$ to the mass of the electric motor $m_{\mathrm{em}}$:

$$m_{\mathrm{em}} = \frac{\Gamma_{\mathrm{m}}}{\Gamma_c}\frac{c_\omega}{r^2} = \frac{\Gamma_{\mathrm{m}}}{\Gamma_c}\frac{(c_{\mathrm{eq}} - c_{\mathrm{s\,eq}})}{(\tau r)^2}. \tag{22}$$

The product $\tau r = \omega r / v_{\mathrm{p}}$ represents the transmission ratio between the linear velocity ($v_{\mathrm{p}}$, in Figure 1) and the tangential speed of the electric motor ($\omega r$). For a given equivalent damping ($c_{\mathrm{eq}}$), motor geometry and materials (this gives $\Gamma_{\mathrm{m}}$ and $\Gamma_c$), the larger this transmission ratio ($\tau r$), the smaller the mass of the electric motor. The apparently unreasonable lower mass corresponding to a larger radius is due to the smaller amount of conductor necessary to obtain the desired damping $c_{\mathrm{eq}}$.

Equations (4), (17), (20) and (22) outline a design procedure of the electromechanical damper.

*Specifications* Definition of the equivalent damping $c_{\mathrm{eq}}$, the maximum force overall mass and bandwidth.

*Design* (1) Decide the motor geometry and materials (this gives $\Gamma_{\mathrm{m}}$ and $\Gamma_c$). Equation (20) gives the equivalent mass ($m_{\mathrm{eq}}$).

(2) Decide the type of mechanical transmission that transforms the linear motion into rotational motion (e.g. ball screw, planetary gear in series to a lever, hydraulic system, etc.). As the size of the transmission is basically a function of the output force or torque, the specifications allow to estimate its mass and mechanical damping $c_{\mathrm{s}}$ at least as a first approximation.

(3) Estimate the mass of the electric motor using Equation (22). The decision about the radius of the electrical machine ($r$) and the transmission ratio ($\tau$) is the key point of the design procedure. Usually, the larger the transmission ratio, the larger the losses within the mechanical system. As these losses include unwanted components of friction type, it is important to keep

the value of $\tau$ as small as possible. To this end, Equation (22) indicates that a relatively small value of $\tau$ corresponds to a larger value of $r$ to limit the mass of the motor. The rotor radius is limited, on the other hand, by the maximum diameter allowed for the electrical machine.

(4) Determine the length of the motor from Equation (17), once the values of $\tau$ and $r$ are decided.

(5) Estimate the overall mass including the contribution of the electric motor and of the transmission.

(6) Assemble the dynamic model of the damper with that of the mechanical system. This allows to understand the overall dynamic behaviour, namely the effects of the added mass and electrical dynamics.

(7) Design the mount stiffness and damping ($k_m$, $c_m$) to limit the transmissibility at high frequency. A guideline in this direction could be to design the mount stiffness to move the resonance $\sqrt{mt/km}$ above the pole frequency $\omega_p$, but below $\omega_0$.

## 4. Example of automotive application: front suspension

The previously outlined procedure has been applied to design the front suspension damper of a C-segment vehicle. The aim is to analyse the potentialities of electromechanical dampers in automotive applications. The relevant specifications are listed in Table 1. Additional specifications are as follows: (1) the suspension layout (Mc Pherson) requires a configuration with structural capabilities. (2) The damper must be connected to the same mechanical interfaces of the conventional one: the wheel hub and the strut mount (upper connection point to the vehicle chassis). (3) Its size must fit in the inner diameter of the coil spring with an appropriate allowance.

With reference to the layout in Figure 5(a), the electromagnetic damper is represented in shade. The electric motor is hosted in the portion with larger diameter close to the upper strut mount. This choice allows to exploit the relatively large diameter inside the spring (8) while keeping a small diameter close to the wheel. The screw (1) is rigidly connected to the moving piston (6), and they are bolted upright in order to limit the not suspended mass. The motor (stator (2), rotor (4) and housing (5)), the nut of the ball screw and the guiding tubes (11) are connected to the unsprung mass. The rotor of the electric motor and the nut of the ball screw are connected together, and this reduces considerably the axial length of the device as it allows exploiting the room inside the rotor of the motor. Ball bearings (3a and 3b), bushings (7a and 7b), coil spring support (10) and rubber spring (9) complete the mechanical configuration.

The damper has been designed following the procedure outlined in Section 3. The most relevant parameters of the design are listed in Table A1. For what the motor is concerned, the

Table 1. Specifications of the damper and parameters of the single-corner suspension.

| | | | |
|---|---|---|---|
| Max damping coefficient (rebound) | $c_{eqmax}$ | >10 | kN s/m |
| Max speed | $v_{max}$ | 1 | m/s |
| Max stroke (pk-pk) | | 150 | mm |
| Spring stiffness | $K_s$ | 18 | kN/m |
| Tire radial stiffness | $K_p$ | 150 | kN/m |
| Tire radial damping | $c_p$ | 50 | Ns/m |
| Suspended mass | $m_s$ | 450 | kg |
| Not suspended mass | $m_{ns}$ | 30 | kg |
| Axial length at mid-stroke | | 450 | mm |
| Max force | $F_{max}$ | 1.8 | kN |

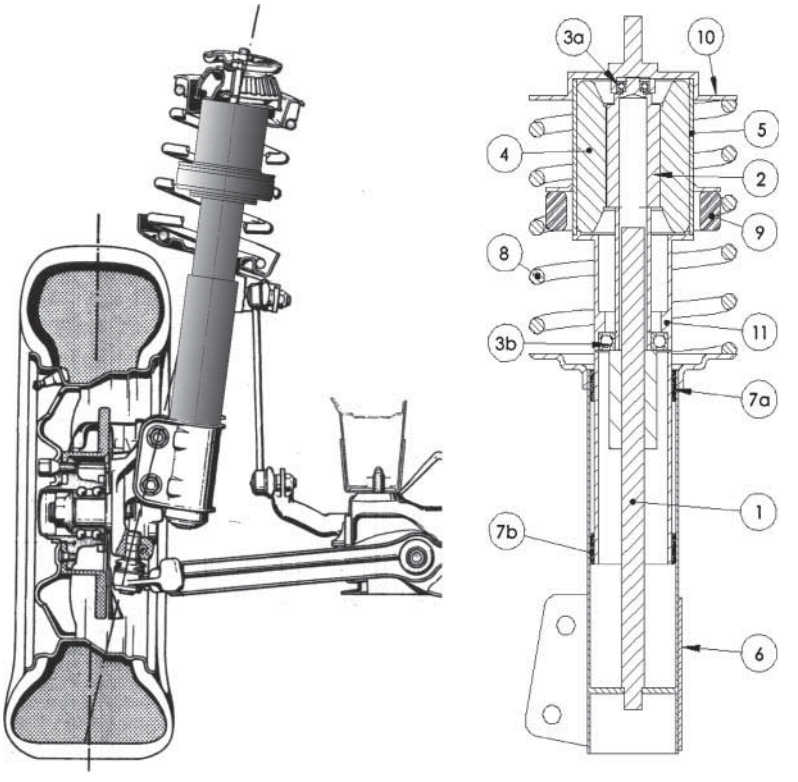


Figure 5. Electromechanical damper integrated in a McPherson suspension and cross section of the damper (right).

geometrical shape factors and the materials have been selected in order to maximise coefficient $\Gamma_c$ and minimise $\Gamma_m$ of Equations (17) and (21). A motor with surface mounted N42 grade – NdFeB PMs has been adopted to this end. A ball screw with a relatively large pitch of 30 mm compared with the diameter of 15 mm has been selected to reduce the mechanical losses and minimise the mass and moments of inertia added by the rotating part of the screw. The design allows to obtain a maximum damping coefficient of $c_{\mathrm{eq\,max}} = 12.1\,\mathrm{kN\,s/m}$ with short circuited phases. Smaller values of the damping can be obtained by adding an external resistance in series with the motor phases. The electrical pole frequency, and the zero frequency and the zero damping factor of the mechanical impedance are $\omega_p = 53\,\mathrm{Hz}$, $\omega_{0m} = 717\,\mathrm{Hz}$, $\omega_{0\mathrm{em}} = 153\,\mathrm{Hz}$, and $\zeta_{0\mathrm{em}} = 0.174$ (Equations (7) and (9)). These values are obtained with short circuited phases (no external resistance: $R_{\mathrm{ext}} = 0$). The force produced by the damper for constant speed deformation is represented in Figure 6, and the different curves are relative to the values of the external resistance in series with the motor phases between 0 and 50Ω. For low speed, the larger the resistance, the lower the slope, but also the larger is the speed corresponding to the maximum of the curve. The result is that all curves are characterised by the same maximum force. The dashed curves with circle markers are relative to a commercial hydraulic damper with continuously variable characteristic adopted for the same vehicle. The force range generated by the electromechanical damper covers the whole range of the hydraulic solution. For small positive speeds (extension, first quadrant $0 < v < 0.1\,\mathrm{m/s}$), the short circuited electromechanical damper ($R_{\mathrm{ext}} = 0$) well approximates the hydraulic characteristic with higher damping. The change in the slope of the same characteristic of the hydraulic damper ($v > 0.1\,\mathrm{m/s}$) can be synthesised by increasing the shunt resistance. A suitable modulation of the resistance can lead to a force–speed characteristic

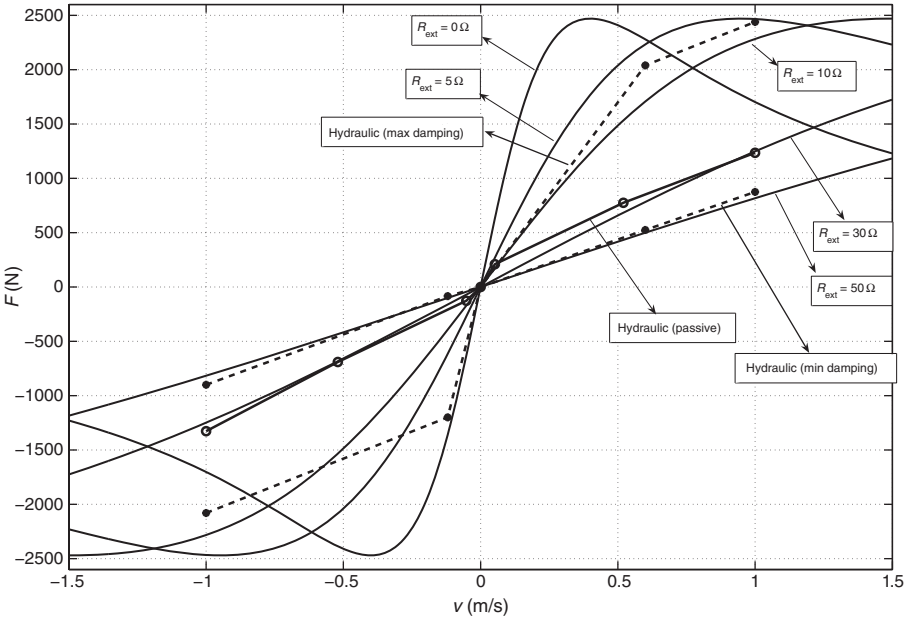


Figure 6. Force-to-speed characteristic of the electromechanical damper. The curves correspond to increasing values of the resistance in series with the winding ($R_{\text{ext}}$).

that inverts its slopes for speeds higher than a given threshold, that is, a regressive characteristic. The same close fit between hydraulic and electromechanical characteristics also applies among the curve with $R_{\text{ext}} = 50\,\Omega$ and the hydraulic characteristic of smaller damping.

The mechanical impedance of the same damper is reported in Figure 7. The constant low-frequency value corresponds to the static damping. This value decreases with an increase in the shunt resistance ($R_{\text{ext}}$). By converse, at high frequency, the inertia locks the rotating parts and the mechanical impedance reduces to the viscous damping coefficient of the mount $c_{\text{m}}$. At

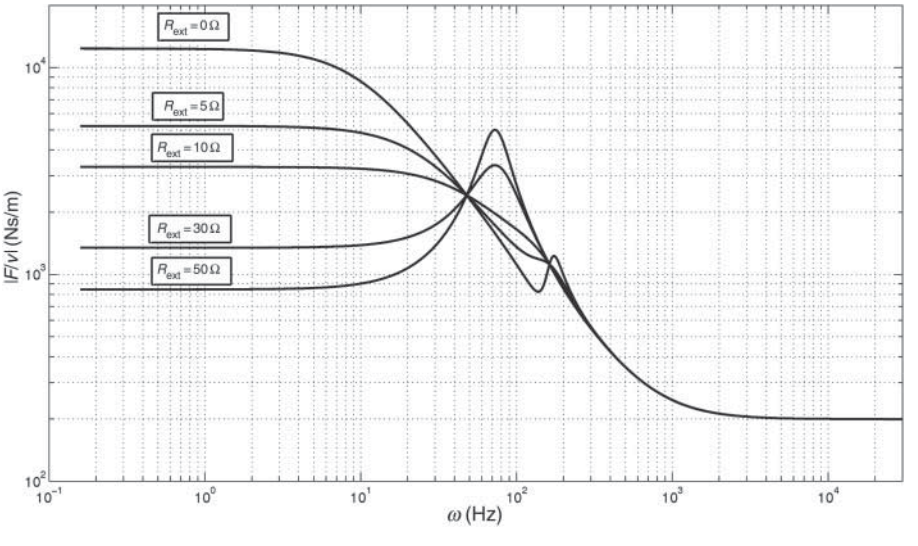


Figure 7. Mechanical impedance of the electromechanical damper for different shunt resistances ($R_{\text{ext}}$).

Table 2. Performance comparison between different passive damper configurations, performances are shown using the damping-to-weight ratio.

| Type | Technology | $\frac{\text{Damping}}{\text{Weight}}\left[\frac{\text{N·s}}{\text{m·kg}}\right]$ |
|---|---|---|
| Conventional | Hydraulic | 2440 |
| Ebrahimi *et al.* [14] | PMs in a conductive tube | 580 |
| Linear motor | Passively shunted commercial linear motor | 490 |
| Proposed solution | Shunted PM motor and ball screw | 2000 |



intermediate frequencies, the impedance is affected first by the electrical pole and then by the mechanical resonance due to the mount stiffness and the equivalent mass ($m_{\text{eq}}$) of the moving parts. The modal damping of this resonance is high for low values of the shunt resistance, and it decreases with increasing values of the shunt resistance. It is worth noting that all curves have two common points at about 50 and 150 Hz. This is similar to other cases related to suspensions with variable damping.

The device has not been manufactured yet, and the overall mass of the damper, estimated by means of the CAD model, is 5 kg. This mass has to be compared with the 4.1 kg of the existing hydraulic solution with continuously variable damping. The proposed damper is still heavier than the hydraulic one, but it is much lighter than the configurations found in the literature with comparable performances. Table 2 shows a comparison between the different concepts by means of the damping-to-weight ratio. An industrial linear motor (LINMOT P01-48x240) with comparable stroke (180 mm) has also been introduced by evaluating its passive damping performances supposing that the terminals are shunted.

As the mechanical energy is dissipated (in part or all) in the electric motor, the temperature could increase above the ranges allowed by the windings and the PMs. Similar to other electrical machines, the solution is to provide the system with an adequate level of thermal dissipation. Looking at the force to velocity curves in Figure 6, the peak power of the damper is in the range of 2.5 kW (2500 N, 1 m/s). Regardless of this, the mean dissipated power dissipated is in the range of 200–300 W, and this is compatible in conventional dampers with a maximum temperature in the fluid of less than 130°C. As similar maximum temperatures apply for the copper and PM materials, the thermal design of the electromagnetic damper should obtain dissipations similar to that of the conventional dampers. Although a dedicated thermal analysis has not been performed yet, the previous considerations seem to indicate that the cooling system could be based on the convection through the outer surface.

## 5. Conclusions

A methodology for the design of passive or semi-active electromechanical dampers has been presented in this paper. The study is motivated by the fact that similar devices proposed in the literature are characterised by an excessive weight. The large weight constitutes one of the strongest reasons against their application in the automotive field. The aim of the design methodology is to obtain a considerable reduction of the weight. To this end, a configuration of the damper based on a rotational electric motor with NdFeB PMs has been considered due to the high torque and power density that characterise these electrical machines. The rotation of the motor is then transformed into linear motion by means of a mechanical or hydraulic transmission, for example, of a ball screw, a lever or an hydraulic system. The methodology is based on the study of the electromechanical damper behaviour including its mechanical

and electrical dynamics. It evidences that the design is driven by a few parameters involving the mechanical and the electrical variables. The application of the design methodology to a C-segment vehicle suspension leads to a solution about 20% heavier mass than a continuously variable hydraulic damper. This is considered a good result. As a matter of fact, the solutions proposed in the literature for similar specifications lead to devices whose mass is usually several times heavier.

Considering that electromechanical dampers allow to avoid a number of drawbacks related to hydraulic ones (effects of the temperature, ageing, cavitation, frequency, etc.), in our opinion, the higher cost of the proposed solution could be justified in applications where performances and reliability issues are of better concern than cost reduction.



## Acknowledgements

This study was sponsored at the Mechatronics Laboratory of Politecnico di Torino by the FIAT Auto company under the capable direction of Ing. Stefano Re Fiorentin and Ing. Guglielmo Caviasso. Their contributions to this work are gratefully acknowledged.

## References

[1] G. Genta, *Motor Vehicle Dynamics: Modeling and Simulation*, World Scientific, Singapore, 1997.
[2] D. Karnopp, *Vehicle Stability*, Marcel Dekker, New York, 2004.
[3] J. Reimpell and H. Stoll, *The Automotive Chassis: Engineering Principles*, SAE International, Warrendale, PA, 1996.
[4] A.L. Audenino and G. Belingardi, *Modelling the dynamic behaviour of a motorcycle damper*, Proc. Inst. Mech. Eng. D J. Automob. Eng. 209(4) (1995), pp. 249–262.
[5] A.C.M. van der Knaap, P.J.T. Venhovens, and H.B. Pacejka, *Evaluation and Practical Implementation of a Low Power Attitude and Vibration Control System*, Proceedings of the International Symposium on Advanced Vehicle Control (AVEC'94), JSAE 9438466, Nagoyo, JP, 1994.
[6] A.C.M. van der Knaap and H.B. Pacejka, *Mass spring system with roll/pitch stabilization for use in vehicles*, International Publication nr. WO93/22150, International patent application nr. PCT/NL93/00094 Rotterdam, NL, 1993.
[7] D.A. Weeks, D.A. Bresie, J.H. Beno, and A.M. Guenin, *The design of an electromagnetic linear actuator for an active suspension*, SAE 1999-01-0730, Detroit, MI, USA, 1999, pp. 1264–1274.
[8] D.A. Weeks, J.H. Beno, A.M. Guenio, and D.A. Bresie, *Electromechanical active suspension demonstration for off-road vehicles*, SAE transactions (SAE2000-01-0102), Detroit, MI, USA, 2000.
[9] D.L. Miller, *Semi-active control of wheel hop in ground vehicles*, Veh. Syst. Dyn. 12 (1983), pp. 317–330.
[10] M.R. Jolly and D.L. Margolis, *Regenerative systems for vibration control*, ASME J. Vib. Acoust. 119 (1997), pp. 208–215.
[11] D. Karnopp, *Force generation in semi-active suspensions using modulated dissipative elements*, Veh. Syst. Dyn. 16 (1987), pp. 333–343.
[12] D. Karnopp, *Permanent magnets linear motors used as variable mechanical dampers for vehicle suspensions*, Veh. Syst. Dyn. 18 (1989), pp. 187–200.
[13] T. Inoue, Y. Ishida, and M. Sumi, *Vibration suppression using electromagnetic resonant shunt damper*, J. Vib. Acoust. 130 (2008), pp. 014003-1–041003-8.
[14] B. Ebrahimi, M.B. Khamesee, and F. Golnaraghi, *Eddy current damper feasibility in automobile suspension: Modeling, simulation and testing*, Smart Mater. Struct. IOP 18 (2009), pp. 015017-1–015017-12.
[15] J.S. Bae, J.H. Hwang, J.S. Park, and D.G. Kwag, *Modeling and experiments on eddy current damping caused by a permanent magnet in a conductive tube*, J. Mech. Sci. Technol. 23 (2010), pp. 3024–3035.
[16] K. Hio, M. Sato, and T. Uno, *Electromagnetic suspension system for vehicle*, U.S. Patent Publication Application, US 2004/0150361 A1, Washington, MD, USA, 2004.
[17] N. Amati, S. Carabelli, F. Cavalli, A. Festini, and A. Tonoli, *Suspension system for a wheeled vehicle and a wheeled vehicle equipped with such a suspension system*, European Patent Application, 060140608.1, Torino, IT, 2006.
[18] A. Tonoli, *Dynamic characteristics of eddy current dampers and couplers*, J. Sound Vib. 301(3–5) (2007), pp. 576–591.
[19] N. Amati, A. Canova, F. Cavalli, S. Carabelli, A. Festini, A. Tonoli and G. Caviasso, *Electromagnetic Shock Absorbers for Automotive Suspensions: Electromechanical Design*, Proceedings of the ASME-ESDA 2006 Conference, Torino, IT, 2006.
[20] J. Meisel, *Principles of Electromechanical Energy Conversion*, Robert Krieger, Malabar, FL, 1984.
[21] T.J.E. Miller, *Brushless Permanent-Magnet and Reluctance Motor Drives*, Clarendon Press, Oxford, 1989.

## Appendix 1. List of symbols and damper parameters

Table A1. Main characteristics of the electromechanical damper.

| | | | |
|---|---|---|---|
| Type of motor | | SMPM | |
| Magnetic material type | | NdFB | N42 grade |
| Number of poles | $p$ | 8 | |
| Number of slots | $N_s$ | 24 | |
| Motor torsional damping parameter | $\Gamma_c$ | $41.3 \times 10^6$ | $\mathrm{N\,m^{-4}\,s/rad}$ |
| Motor mass parameter | $\Gamma_m$ | $7.98 \times 10^4$ | $\mathrm{kg/m^3}$ |
| Phase resistance | $R$ | 3.65 | Ω |
| Phase inductance | $L$ | 10.9 | mH |
| Torque constant | $K_t$ | 1.242 | Nm/A |
| Back emf constant | $K_e$ | 0.828 | Vs/rad |
| Rotor active length | $l$ | 65 | mm |
| Rotor radius | $r$ | 18 | mm |
| Rotor moment of inertia | $J_{em}$ | 75 | $\mathrm{kg\,mm^2}$ |
| Stator outer diameter | | 76 | mm |
| Air gap width | $\delta$ | 0.5 | mm |
| Motor weight | $m_{em}$ | 1.68 | kg |
| Screw pitch | $1/\tau$ | 30 | mm/rev |
| Screw diameter | | 15 | mm |
| Screw dynamic load | | 10 | kN |
| Total mass of the damper | | 5 | kg |
| Moment of inertia of rotor | $J$ | 26 | $\mathrm{kg\,mm^2}$ |

## Appendix 2. Electromechanical coefficients

Figure A1 shows a schematic representation of the slots and teeth geometry with the relevant dimensions. The present design procedure is based on a number of aspect ratios between the geometrical dimensions. With reference to Figure A1, they are defined as follows:

$$K_{st} = \frac{W_s}{W_t} \quad K_s = \frac{W_{\delta s}}{W_s},$$

$$K_{sy} = \frac{H_s}{H_y} \quad K_t = \frac{W_{\delta t}}{W_t}, \tag{A1}$$

$$K_y = \frac{H_y}{W_t} \quad K_r : \text{slot filling factor},$$

$$H = \frac{K_{sy} K_y K_r K_{st}}{(K_s K_{st} + K_t)^2}, \tag{A2}$$

$$K_{conn.} = \frac{l_{cu}}{2l} = 1 + 5\frac{r+\delta}{pl}. \tag{A3}$$

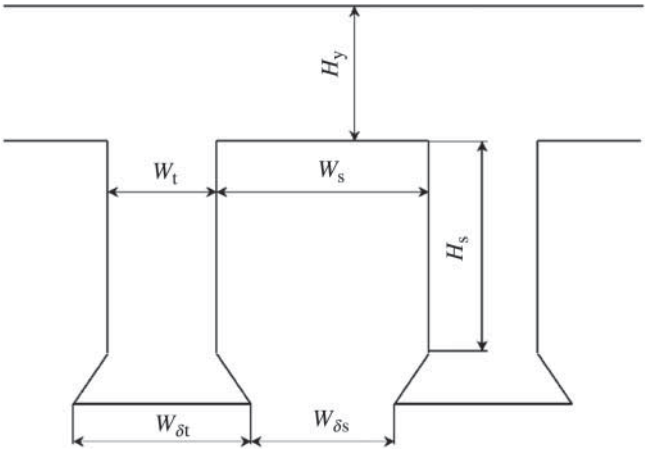


Figure A1. Layout of the teeth and slot of the stator with main geometric dimensions.